The Constancy of the Constants of Nature: Updates

Takeshi Chiba

Department of Physics, College of Humanities and Sciences, Nihon University, Tokyo 156-8550, Japan

The current observational and experimental bounds on time variation of the constants of nature (the fine structure constant α, the gravitational constant G and the proton-electron mass ratio $\mu = m_p/m_e$) are reviewed.

arXiv:1111.0092v1 [gr-qc] 1 Nov 2011

§1. Introduction

The title of this paper is oxymoron. We mean the title as the possibility of variation of the quantities which are supposed to be constants.

There are two aspects of the constants of nature: the system of units and the laws of nature. On the one hand, when we attempt to describe natural phenomena using physics laws, physical quantities are expressed using physical constants: the speed of light c, Planck (Dirac) constant $h(\hbar)$, the gravitational constant G, Boltzmann constant k, electron (proton) mass $m_e(m_p)$, for example. When combined these constants with the electric constant ϵ_0, we can determine all the units in the SI units. On the other hand, there are four fundamental forces in nature: electromagnetic, weak, strong, gravitational. The coupling constants which describe the strength of these forces are physical constants of fundamental importance: the fine structure constant $\alpha = e^2/4\pi\epsilon_0\hbar c \simeq 7.30 \times 10^{-3} \simeq 1/137$, the Fermi coupling constant $G_F/(\hbar c)^3 \simeq 1.17 \times 10^{-5}\mathrm{GeV}^{-2}$, the strong coupling constant $\alpha_S \simeq 0.119$, the gravitational constant $G \simeq 6.67 \times 10^{-11}\mathrm{m}^3\mathrm{kg}^{-1}\mathrm{s}^{-2}$. A dimensionless gravitational fine structure constant $\alpha_G = Gm_p^2/\hbar c \simeq 5.10 \times 10^{-39}$ is also useful. Therefore, if these constants are not constant, then the correspondence between the experimental results and theories would depend on when and where the measurements are performed, which would results in the violation of the universality of the laws of nature. Testing the constancy of the physical constants thus has fundamental importance.

1.1. *Large Number Hypothesis*

Dirac appears to have been the first who argued for the possibility of time variation of the constants of nature.[2)] As is well-known, dimensionless numbers involving G are huge (or minuscule). For example, the ratio of the electrostatic force to the gravitational force between an electron and a proton is

$$N_1 = \frac{e^2}{Gm_p m_e} \simeq 2 \times 10^{39}, \tag{1·1}$$

where e is the electric charge, m_p is the proton mass and m_e is the electron mass. Similarly, the ratio of the Hubble horizon radius of the Universe, H_0^{-1} to the classical

radius of an electron is

$$N_2 = \frac{cH_0^{-1}}{e^2 m_e^{-1} c^{-2}} \simeq 3 \times 10^{40} h^{-1}, \tag{1·2}$$

where h is the Hubble parameter in units of $100\mathrm{kms}^{-1}\mathrm{Mpc}^{-1}$. Curiously, the two nearly coincide, which motivated Dirac to postulate the so-called the large number hypothesis 1). In his article entitled "A new basis for cosmology", he describes 1)

> *Any two of the very large dimensionless numbers occurring in Nature are connected by a simple mathematical relation, in which the coefficients are of the order of magnitude unity.*

Thus if the (almost) equality $N_1 = \mathcal{O}(1) \times N_2$ holds always, then G must decrease with time $G \propto t^{-1}$2), or the fine structure constant, $\alpha \equiv e^2$, must increase with time $\alpha \propto t^{1/2}$ 3) since $H \propto t^{-1}$.

Nowadays we know that such a huge dimensionless number like N_1 is related to the gauge hierarchy problem. In fact, the gauge couplings are *running* (however, only logarithmically) as the energy grows, and all the gauge couplings are believed to unify at the fundamental energy scale (probably string scale). The fact that N_1 nearly coincides with N_2 may be just accidental, and pursuing the relation between them is numerological speculation (or requires anthropic arguments). However, Pandora's box was opened. In the following, we mention several motivations for considering the variation of the constants of nature.

1.2. *Newton, Einstein, String*

Space and time in Newtonian mechanics are rigid and immutable: the absolute space and time which define the absolute inertial frame and exist forever even without matter.

The concept of space and time in general relativity is different. The structure of space and time is affected by the presence of matter and thus becomes soft and malleable. However, the laws of physics are kept rigid: the equivalence principle fixes locally the laws of physics.

On the other hand, string theory can be viewed as a framework for softening the laws of physics 4). In string theory, the coupling constants are determined by the vacuum expectation values of some scalar fields and thus they are no longer constant at all. The situation is summarized in Table I.

	spacetime	laws of physics
Newton	rigid	rigid
Einstein	soft	rigid
String Theory	soft	soft

Table I. Softening of Spacetime and Laws of Physics

String theory is the most promising approach to unify all fundamental forces in nature. It is believed that in string theory all the coupling constants and parameters (except the string tension) in nature are derived quantities and are determined by the vacuum expectation values of the dilaton and moduli. However, no compelling mechanism how and when to fix the dilaton/moduli is known.

On the other hand, we know that the Universe is expanding. Then it is no wonder to imagine the possibility of time variation of the constants of nature during the evolution of the Universe.

In fact, it is argued that the effective potentials of dilaton or moduli induced by nonperturbative effects may exhibit runaway structure; they asymptote zero for the weak coupling limit where dilaton becomes minus infinity or internal radius becomes infinity and symmetries are restored in the limit 5), 6). Thus it is expected that as these fields vary, the natural "constants" may change in time and moreover the violation of the weak equivalence principle may be induced 6), 7) (see also 8), 9) for earlier discussion).

Hence, any detection or nondetection of such variations at various cosmological epochs could provide useful information about the nature of moduli fixing and the coupling of the quintessence field.

1.3. *Importance as Null Tests*

We should emphasize another important aspect of checking the constancy of the fundamental constants: a null test. It is of fundamental importance to check to what extent the gravitational force obeys the inverse square law and to what extent the equivalence principle (the universality of free-fall) holds. Likewise, it is of fundamental importance to check the constancy of the fundamental constants to the ultimate precision. By comparing the experimental values at various epochs and positions, we could confirm the internal consistency of the foundation of the laws of physics.

1.4. *Use of Cosmology*

Cosmological observations have played important roles to test the constancy of the fundamental constants, which may be evident by writing the time derivative in terms of a difference:

$$\frac{\Delta\alpha}{\alpha\Delta t}. \tag{1·3}$$

Therefore, in order to place a strong constraint on the time variability, one needs to (1) measure the constant accurately (thereby minimizing $\Delta\alpha/\alpha$) or to (2) measure for a long time (larger Δt). Laboratory precision experiments correspond to the former ($\Delta\alpha/\alpha \ll 1$ but $\Delta t \sim \mathcal{O}(1)$ yr), while cosmological observations the latter (Δt as much as 137 Gyr but $\Delta\alpha/\alpha \sim \mathcal{O}(1)$).

1.5. *Plan of the Paper*

In this article, we review the current experimental (laboratory, astrophysical and geophysical) constraints on the time variation of the constants of nature. In particular, we consider α (sec.2), G (sec.3), m_p/m_e (sec.4) and Λ (sec.5), extending and updating our previous review 10). More than ten years have passed since our previous review, and significant progress has been made in the experimental constraints on the variation (in particular thanks to the release of the WMAP data), so it is very timely to update our review. See also 13) for recent reviews. For earlier expositions, see 11), 12) for example. We sometimes use the units of $\hbar = c = 1$ and assume

$H_0 = 100h$km/s/Mpc with $h = 0.71$ for the Hubble parameter and $\Omega_M = 0.27$ and $\Omega_\Lambda = 0.73$ for the cosmological parameters taken from WMAP results 14).

§2. α

In this section, we review the experimental constraints on time variation of the fine structure constant. The results are summarized in Table II.

	redshift	$\Delta\alpha/\alpha$	$\dot{\alpha}/\alpha(\mathrm{yr}^{-1})$
Atomic Clock($Yb^+/Hg^+/H$)[60]	0		$(-0.3 \pm 2.0) \times 10^{-15}$
Atomic Clock($Hg^+/Yb^+/H$)[62]	0		$(-0.55 \pm 0.95) \times 10^{-15}$
Atomic Clock($Sr/Hg^+/Hg^+/H$)[63]	0		$(-3.3 \pm 3.0) \times 10^{-16}$
Atomic Clock(Al^+/Hg^+)[65]	0		$(-1.6 \pm 2.3) \times 10^{-17}$
Atomic Clock($^{162}Dy/^{163}Dy$)[68]	0		$(-2.7 \pm 2.6) \times 10^{-15}$
Oklo(Damour-Dyson[16])	0.16	$(-0.9 \sim 1.2) \times 10^{-7}$	$(-6.7 \sim 5.0) \times 10^{-17}$
Oklo(Fujii et al.[17])	0.16	$(-0.18 \sim 0.11) \times 10^{-7}$	$(0.2 \pm 0.8) \times 10^{-17}$
Oklo(Petrov et al.[19])	0.16	$(-0.56 \sim 0.66) \times 10^{-7}$	$(-3.7 \sim 3.1) \times 10^{-17}$
Oklo(Gould et al.[20])	0.16	$(-0.24 \sim 0.11) \times 10^{-7}$	$(-0.61 \sim 1.3) \times 10^{-17}$
Re/Os bound[26]	0.44	$(-0.25 \pm 1.6) \times 10^{-6}$	$(-4.0 \sim 2.9) \times 10^{-14}$
HI 21 cm[31]	1.8	$(3.5 \pm 5.5) \times 10^{-6}$	$(-3.3 \pm 5.2) \times 10^{-16}$
HI 21 cm[32]	0.25,0.68	$< 1.7 \times 10^{-5}$	
QSO absorption line(SiIV)[31]	$2.67 - 3.55$	$< 3.5 \times 10^{-4}$	
QSO absorption line(MM)[33]	$0.5 - 1.6$	$(-1.09 \pm 0.36) \times 10^{-5}$	
QSO absorption line(MM)[34]	$0.5 - 3.5$	$(-0.72 \pm 0.18) \times 10^{-5}$	
QSO absorption line(SiIV)[35]	$2.01 - 3.03$	$(-0.5 \pm 1.3) \times 10^{-5}$	
QSO absorption line(MM)[36]	$0.2 - 3.7$	$(-0.543 \pm 0.116) \times 10^{-5}$	
QSO absorption line(MM)[37]	$0.2 - 4.2$	$(-0.573 \pm 0.113) \times 10^{-5}$	
OH[133]	0.247671	$(0.51 \pm 1.26) \times 10^{-5}$	$(-1.7 \pm 4.3) \times 10^{-15}$
OH[135]	0.247	$(-3.1 \pm 1.2) \times 10^{-6}$	$(1.1 \pm 0.4) \times 10^{-15}$
QSO absorption line(MgII/FeII)[39]	$0.4 - 2.3$	$(-0.06 \pm 0.06) \times 10^{-5}$	
QSO absorption line(MgII/FeII)[47]	$0.4 - 2.3$	$(-0.44 \pm 0.16) \times 10^{-5}$	
QSO absorption line(SiIV)[40]	$1.59 - 2.92$	$(0.15 \pm 0.43) \times 10^{-5}$	
QSO absorption line(FeII)[44]	1.84	$(5.66 \pm 2.67) \times 10^{-6}$	$(-5.51 \pm 2.60) \times 10^{-16}$
QSO absorption line(FeII)[44]	1.15	$(-0.12 \pm 1.79) \times 10^{-6}$	$(0.14 \pm 2.11) \times 10^{-16}$
QSO absorption line(FeII)[45]	1.15	$(0.5 \pm 2.4) \times 10^{-6}$	$(-0.6 \pm 2.8) \times 10^{-16}$
CMB[78]	10^3	$-0.06 \sim 0.01$	$< 5 \times 10^{-12}$
CMB[80]	10^3	$-0.013 \sim 0.015$	$< 1 \times 10^{-12}$
BBN[74]	10^{10}	$< 6 \times 10^{-2}$	$< 4.4 \times 10^{-12}$

Table II. Summary of the experimental bounds on time variation of the fine structure constant. $\Delta\alpha/\alpha \equiv (\alpha_{\rm then} - \alpha_{\rm now})/\alpha_{\rm now}$.

2.1. *Earth and $\dot{\alpha}$: Oklo Natural Reactor and Meteorites*

2.1.1. Oklo Natural Reactor.

In 1972, the French CEA (Commissariat à l'Energie Atomique) discovered ancient natural nuclear reactors in the ore body of the Oklo uranium mine in Gabon, West Africa. It is called the Oklo phenomenon. The reactor operated about 2 bil-

lion years ago corresponding to the redshift $z \simeq 0.16$ for the assumed cosmology ($h = 0.71, \Omega_M = 0.27, \Omega_\Lambda = 0.73$).

Shlyakhter noticed the extremely low resonance energy ($E_r = 97.3$meV) of the reaction

$$^{149}S_m + n \rightarrow {}^{150}S_m + \gamma, \tag{2·1}$$

and hence the abundance of $^{149}S_m$ (one of the nuclear fission products of ^{235}U) observed at the Oklo can be a good probe of the variability of the coupling constants 15). The isotope ratio of $^{149}S_m/{}^{147}S_m$ is 0.02 rather than 0.9 as in natural samarium due to the neutron flux onto $^{149}S_m$ during the uranium fission. The neutron-absorption cross section $\sigma(E)$ of the reaction Eq. (2·1) is well described by the Breit-Wigner formula,

$$\sigma(E) = \frac{g\pi\hbar^2}{2m_n E}\frac{\Gamma_n\Gamma_\gamma}{(E-E_r)^2 + \Gamma^2/4}, \tag{2·2}$$

where g is the statistical factor and $\Gamma = \Gamma_n + \Gamma_\gamma$ is the total width in terms of the neutron and the photon widths. From an analysis of nuclear and geochemical data, the operating conditions of the reactor was inferred and the thermally averaged neutron-absorption cross section could be estimated. The result was $\Delta E_r = E_r^{Oklo} - E_r^0 = (-120 \sim 90)$meV 16) and $\Delta E_r = 4 \pm 16$ meV 17). On the other hand, from the mass formula of heavy nuclei, the change in resonance energy is related to the change in α through the Coulomb energy contribution

$$\Delta E_r = -1.1\frac{\Delta\alpha}{\alpha}\text{MeV}. \tag{2·3}$$

By estimating the uncertainty in the resonance energy, Shlyakhter obtained the famous bound $\dot{\alpha}/\alpha = 10^{-17}\text{yr}^{-1}$. Damour and Dyson reanalyzed the data by carefully estimating the uncertainty and obtained $\dot{\alpha}/\alpha = (-6.7 \sim 5.0) \times 10^{-17}\text{yr}^{-1}$ 16). Using new samples that were carefully collected to minimize natural contamination and also on a careful temperature estimate of the reactors, Fujii et al. reached a tighter bound *) $\dot{\alpha}/\alpha = (0.2 \pm 0.8) \times 10^{-17}\text{yr}^{-1}$ 17).**)

Recently, the use of the Maxwell-Boltzmann distribution for low energy neutron spectrum was questioned and it is claimed that the analysis of Oklo data by employing a more realistic spectrum including the $1/E$ tail implies a decrease in α, $\Delta\alpha/\alpha \geq 4.5 \times 10^{-8}$ with the significance being 6σ 18). Full-scale computations of the Oklo reactor using modern method of reactor physics, however, show no evidence for such a change: $\Delta\alpha/\alpha = (-5.6 \sim 6.6) \times 10^{-8}$ 19); $\Delta\alpha/\alpha = (-2.4 \sim 1.1) \times 10^{-8}$ 20).***) The discrepancy arises because the reactor model used in 18) is an infinite medium reactor model and is found to be undercritical if the reactor is made finite.

*) They noted that data is also consistent with a non-null result: $(-4.9 \pm 0.4) \times 10^{-17}\text{yr}^{-1}$, indicating an apparent evidence for the time variability. However, from the analysis of the isotope compositions of G_d, the consistency of the S_m and G_d results supports the null results.

**) Note the plus sign in front of 0.2 unlike 17) which should be consistent with their value of ΔE_r and the relation Eq.(2·3).

***) Note that in the authors of 20) use the formula Eq.(2·3) with the opposite sign which is corrected here.

2.1.2. Meteorites.

Another geophysical bound on the variation of α can be obtained from the determination of nuclear decay rates using meteoritic data 11), 21). The isotopes which are most sensitive to changes in α are typically those with lowest beta-decay Q-value, Q_β. The isotope with the smallest $Q_\beta (= 2.66 \pm 0.02\text{keV})$ value is ^{187}Re 21).

The present abundances of ^{187}Re and ^{187}Os are given by

$$(\,^{187}\text{Re})_0 = (\,^{187}\text{Re})_i \exp(-\bar{\lambda}(t_0 - t_i)), \tag{2·4}$$

$$(\,^{187}\text{Os})_0 = (\,^{187}\text{Os})_i + (\,^{187}\text{Re})_i \left(1 - \exp(-\bar{\lambda}(t_0 - t_i))\right), \tag{2·5}$$

where the subscripts 0 and i refer to the present and the initial quantities and $\bar{\lambda}$ is the time averaged decay constant: $\bar{\lambda} = \int_{t_i}^{t_0} \lambda(t)dt/(t_0 - t_i)$. $(\,^{187}\text{Re})_i$ can be eliminated to give

$$(\,^{187}\text{Os})_0 = (\,^{187}\text{Os})_i + (\,^{187}\text{Re})_0 \left(\exp(\bar{\lambda}(t_0 - t_i)) - 1\right), \tag{2·6}$$

which provides a linear relation (an isochron) between the present abundances (relative to ^{188}Os) of ^{187}Re and ^{187}Os. The slope of the linear curve determines $\bar{\lambda}$ once the age $t_0 - t_i$ is independently determined.

The ^{187}Re decay constant has been determined through the generation of high precision isochrons from material of known ages, particularly iron meteorites. Using the Re-Os ratios of IIIAB iron meteorites that are thought to have been formed in the early crystallization of asteroidal cores, Smoliar et al. found a ^{187}Re decay constant of $\bar{\lambda} = (1.6666 \pm 0.009) \times 10^{-11}\text{yr}^{-1}$ assuming that the age of the IIIA iron meteorites is $4.5578\text{Gyr} \pm 0.4\text{Myr}$ which is identical to the Pb-Pb age of angrite meteorites 22) *).

The beta-decay constant depends on Q_β as $\lambda \propto Q_\beta^{2.835}$ 23), and if we assume that the variation of Q_β comes entirely from the Coulomb term, we find using the nuclear mass formula 24) that $\Delta Q_\beta = -19\text{MeV}\Delta\alpha/\alpha$. Hence,

$$\frac{\Delta\lambda}{\lambda} = -2.0 \times 10^4 \frac{\Delta\alpha}{\alpha}. \tag{2·7}$$

The bound on $\Delta\alpha/\alpha$ over the age of the solar system $\simeq 4.6\text{Gyr}$ ($z \simeq 0.44$) is thus obtained from the comparison of the ^{187}Re meteoritic measurements of the time averaged ^{187}Re decay rate with the recent laboratory measurements 25) : $\Delta\alpha/\alpha = (2.5 \pm 16) \times 10^{-7}$ at $z \simeq 0.44$ 26).**) The difference between 26) and 27) comes from the difference in the adopted laboratory measurements of the decay rate. We use a more recent measurement 25). It is to be noted, however, that the bound depends on the way of time dependence of the ^{187}Re decay constant 26).

*) Note that the authors of 22) recommend the value of $\lambda = (1.6666 \pm 0.017) \times 10^{-11}\text{yr}^{-1}$ considering the systematic error associated with the spike calibration (see Ref.16 in 22)).

**) We take the recommended value of λ for the meteorites. Even if we assume 0.5% error for the meteoritic measurements, the bound only becomes $\Delta\alpha/\alpha = (-2.5 \pm 15) \times 10^{-7}$.

2.2. *(Hyper)Fine splitting and $\dot{\alpha}$*

According to the Dirac equation, the energy levels of a hydrogen-like atom with atomic number Z are given by

$$\begin{aligned} E_{nj} &= \frac{m_e c^2}{\sqrt{1 + Z^2\alpha^2/(n-\delta_j)^2}} \\ &= m_e c^2 - \frac{m_e c^2 Z^2 \alpha^2}{2n^2} - \frac{m_e c^2 Z^4 \alpha^4}{n^3(2j+1)} + \frac{3 m_e c^2 Z^4 \alpha^4}{8n^4} + \ldots, \end{aligned} \tag{2·8}$$

where $\delta_j = j + \frac{1}{2} - \sqrt{(j+\frac{1}{2})^2 - Z^2\alpha^2}$, n is the principal quantum number and j is the quantum number associated with the total electron angular momentum. The fine structure, which arises due to the spin-orbit coupling, is the difference in energy between levels of different j for the same n. For example, for the hydrogen atom, $E(2P_{3/2}) - E(2P_{1/2}) \simeq m_e c^2 \alpha^4/32 \simeq 4.53 \times 10^{-5}\mathrm{eV} \simeq hc/(2.75\mathrm{cm})$. The energy levels are further split into doublets (hyperfine structure) by the coupling of the proton spin with the total electron angular momentum. For example, for the hydrogen atom, the hyperfine splitting for s states ($n = 1, j = 1/2$) is given by[28] $\Delta E_{hf} = \frac{4}{3} m_e c^2 \alpha^4 \frac{m_e}{m_p} g_p \simeq 5.89 \times 10^{-6}\mathrm{eV} \simeq hc/(21.1\mathrm{cm})$, where g_p is the proton gyromagnetic ratio.

Since the fine structure levels depend on α, the wavelength spectra of cosmologically distant quasars provide a natural laboratory for investigating the time variability of α. Narrow lines in quasar spectra are produced by absorption of radiation in intervening clouds of gas, many of which are enriched with heavy elements. Because quasar spectra contain doublet absorption lines at a number of redshifts, it is possible to check for time variation in α simply by looking for changes in the doublet separation of alkaline-type ions with one outer electron as a function of redshift 29), 30). By looking at Si IV doublet, Cowie and Songaila obtained the constraint up to $z \simeq 3$: $|\Delta\alpha/\alpha| < 3.5 \times 10^{-4}$ 31). Also by comparing the hyperfine 21 cm HI transition with optical atomic transitions in the same cloud at $z \simeq 1.8$, they obtained a bound on the fractional change in α up to redshift $z \simeq 1.8$: $\Delta\alpha/\alpha = (\alpha_{z=1.8} - \alpha_0)/\alpha = (3.5 \pm 5.5) \times 10^{-6}$, corresponding to $\dot{\alpha}/\alpha = (-3.3 \pm 5.2) \times 10^{-16}\mathrm{yr}^{-1}$ 31). Recently, by comparing the absorption by the HI 21 cm hyperfine transition (at $z = 0.25, 0.68$) with the absorption by molecular rotational transitions, Carilli et al. obtained a bound: $|\Delta\alpha/\alpha| < 1.7 \times 10^{-5}$ 32).

Webb et al. 33) introduced a new technique (called many-multiplet method) that compares the absorption wavelengths of magnesium and iron atoms in the same absorbing cloud, which is far more sensitive to a change in α than the alkaline-doublet method. They observed a number of intergalactic clouds at redshifts from 0.5 to 1.6. For the entire sample (30 absorption systems) they find $\Delta\alpha/\alpha = (-1.09 \pm 0.36) \times 10^{-5}$, deviating from zero at the 3 σ. They noted that the deviation is dominated by measurements at $z > 1$, where $\Delta\alpha/\alpha = (-1.9 \pm 0.5) \times 10^{-5}$.

Moreover, Webb et al. 34) presented further evidence for time variation of α by reanalyzing the previous data and including new sample of Keck/HIRES (High Resolution Echelle Spectrometer) absorption systems. The results indicate a smaller α in the past and the optical sample (72 systems) shows a 4 σ deviation for $0.5 <$

$z < 3.5$: $\Delta\alpha/\alpha = (-0.72 \pm 0.18) \times 10^{-5}$. They noted that the potentially significant systematic effects only make the deviation significant.

The latest analysis of the third sample including 128 absorption systems for $0.2 < z < 3.7$, gives $\Delta\alpha/\alpha = (-0.543 \pm 0.116) \times 10^{-5}$ 36), and the sample is slightly updated to 143 absorption systems in 37) to yield $\Delta\alpha/\alpha = (-0.573 \pm 0.113) \times 10^{-5}$ for $0.2 < z < 4.2$. Again it is consistent with a smaller α in the past. The significance is now 4.7 σ.

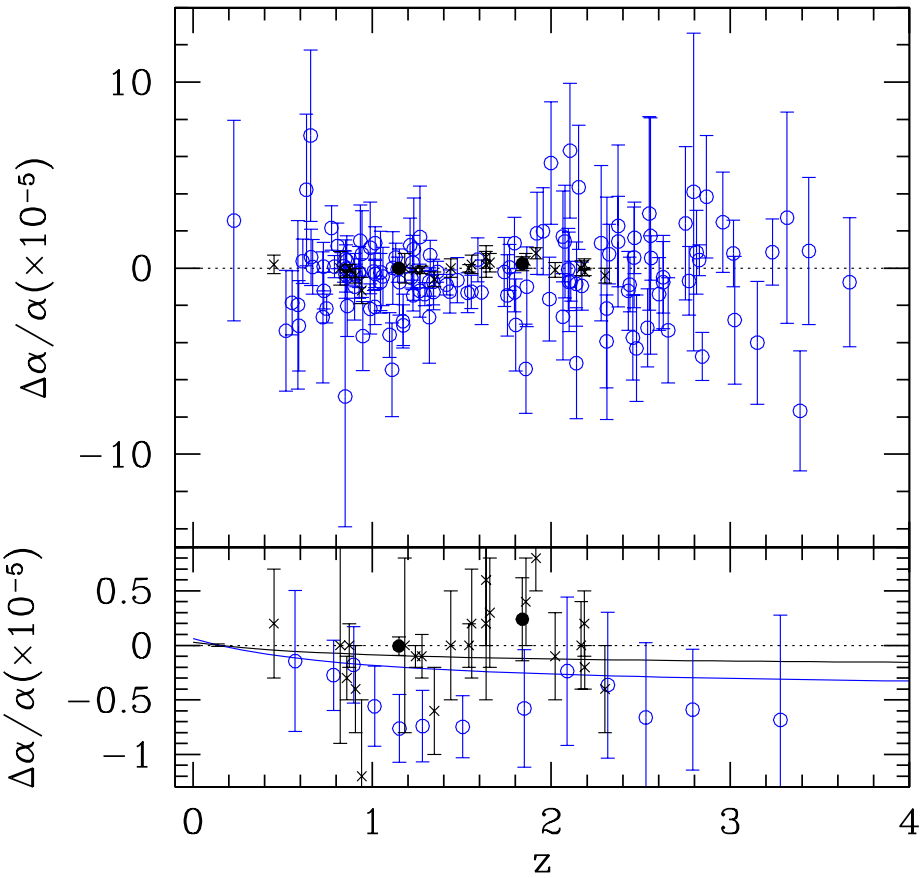

Fig. 1. The fine structure constant determined by quasar absorption lines at several redshifts. Open (blue) circles are the data from 33), 34), 36)(Keck) and crosses are from 39) (VLT) filled circles are from 42), 43) (VLT). The lower panel is the binned data of 33), 34), 36) and the value of $\Delta\alpha/\alpha$ in each bin is the weighted mean with its associated 1σ error bar. The datum at $z \simeq 0.14$ is the Oklo bound 16). A curve is a linear (in scale factor) fit to the data: $\Delta\alpha/\alpha = 2.93 \times 10^{-7} - 2.31 \times 10^{-6}(1-a)$. A blue curve is a fit using 47) instead of 39) : $\Delta\alpha/\alpha = 6.08(\pm 2.22) \times 10^{-7} - 4.85(\pm 1.46) \times 10^{-6}(1-a)$.

More recently, Webb et al. analyzed a dataset from the ESO Very Large Telescope (VLT) and found the opposite trend: α was *larger* in the past 38). Combined

with the Keck samples, they claimed the *spatial* variation of α 38) :

$$\frac{\Delta\alpha}{\alpha} = (1.10 \pm 0.25) \times 10^{-6} (r/\mathrm{Glyr}) \cos\theta, \tag{2·9}$$

where r is the look-back time $r = ct(z)$ and θ is the angle between the direction of the measurement and the axis of best-fit dipole.

If these observational results are correct, it would have profound implications for our understanding of fundamental physics. So the claim needs to be verified independently by other observations. However, recent observations from VLT/UVES (Ultraviolet and Visual Echelle Spectrograph) using the same MM method (but only single species) have not been able to duplicate these results: for one group, $\Delta\alpha/\alpha = (-0.06 \pm 0.06) \times 10^{-5}$ for MgII/FeII systems at $0.4 < z < 2.3$ 39) and $\Delta\alpha/\alpha = (0.15 \pm 0.43) \times 10^{-5}$ for SiIV systems at $1.59 \leq z \leq 2.92$ 40), while for another group, $\Delta\alpha/\alpha = (-0.04 \pm 0.46) \times 10^{-5}$ for FeII systems at $z = 1.15$ 41). Recently, in order to avoid the influence of spectral shifts due to ionization inhomogeneities in the absorbers and non-zero offsets between different exposures, a new method of probing variability of α using pairs of FeII lines observed in individual exposures (called SIDAM, for single ion differential α measurement procedure) is proposed 42), 43). Using this method, a tighter bound is obtained: for FeII systems at $z = 1.839$, $\Delta\alpha/\alpha = (5.66 \pm 2.67) \times 10^{-6}$ 44) and $\Delta\alpha/\alpha = (-0.12 \pm 1.79) \times 10^{-6}$ for FeII at $z = 1.15$ 44). The data taken by another spectrograph HARPS mounted on VLT gives similar bound: $\Delta\alpha/\alpha = (0.05 \pm 0.24) \times 10^{-5}$ for the same FeII systems at $z = 1.1508$ 45).

It is to be noted, however, that the analysis by Srianand et al. 39) seems suffer from several flaws 46) : only about half of the observations analyzed in Chand et al. 39) have calibration spectra taken before and after the object exposure, although in their paper they mentioned that procedure has been followed for all the spectra. Moreover, the uncertainty in wavelength calibration in 39) may not be consistent with the error in $\Delta\alpha/\alpha$ 42). According to the analysis of the fundamental noise limitation 42), the systematic errors in 39) may be several times underestimated. Recent detailed re-analysis of Srianand et al. and Chand et al. confirms these concerns: flawed parameter estimation methods in a χ^2 minimization analysis 47) (see however, 48)) and systematic errors in the UVES wavelength calibration 49) *). Revised value correcting for respective error is $\Delta\alpha/\alpha = (-0.44 \pm 0.16) \times 10^{-5}$ (χ^2 minimization) 47) and $\Delta\alpha/\alpha = (-0.17 \pm 0.06) \times 10^{-5}$ (wavelength calibration) 49).

The data taken from Keck and VLT are shown in Fig. 1. A curve is a linear (in scale factor) fit to the data: $\Delta\alpha/\alpha = 2.93(\pm 1.80) \times 10^{-7} - 2.31(\pm 1.01) \times 10^{-6}(1-a)$ and the reduced χ^2 is $\chi^2/\mathrm{d.o.f} = 1.15$ **).

We have observed the same objects as Webb et al.'s group by Subaru telescope on August 2004 52). The analysis of our observations would provide another inde-

*) Recently, systematic errors in the absolute wavelength calibration of the optical spectrum of HIRES are identified in 50) with typical amplitudes being ± 250m/s. However, their effects on $\Delta\alpha/\alpha$ are found to be relatively small 51): from $(-0.57 \pm 0.11) \times 10^{-5}$ to $(-0.61 \pm 0.11) \times 10^{-5}$.

**) If we use 47) instead of 39), the corresponding fitting curve is $\Delta\alpha/\alpha = 6.08(\pm 2.22) \times 10^{-7} - 4.85(\pm 1.46) \times 10^{-6}(1-a)$ (blue curve in lower panel of Fig. 1.) and the reduced χ^2 is $\chi^2/\mathrm{d.o.f} = 1.53$.

pendent useful information and help to clarify the situation.

2.3. *Laboratory Tests: Clock Comparison*

Laboratory experiments place constraints on present day variation of α and are repeatable and systematic uncertainties can be studied by changing experimental conditions, and hence such laboratory experiments are complementary to the geophysical or cosmological measurements. The laboratory constraints so far are based on comparisons of atomic clocks with ultrastable oscillators of different physical makeup such as the superconducting cavity oscillator vs. the cesium hyperfine clock transition 53) or the Mg fine structure transition vs. the cesium hyperfine clock transition 54). In S.I units, the second is defined as "the duration of 9192631770 periods of the radiation corresponding to the transition between the two hyperfine levels of the ground state of the ^{133}Cs atom" 55). A cesium atomic clock is the apparatus which tune the microwave oscillator to the same frequency as the resonant absorption frequency of cesium (9192631770Hz). Such a clock comparison can be a probe of time variation of α since a hyperfine splitting is a function of $Z\alpha$ (Z is an atomic number) and is proportional to $Z\alpha^2(\mu_N/\mu_B)(m_e/m_p)R_\infty F_{rel}(Z\alpha)$ (where $F_{rel}(Z\alpha)$ is the relativistic correction factor, μ_N is the nuclear magnetic moment, $\mu_B = e\hbar/2m_pc$ is the nuclear magneton, and $R_\infty = \alpha^2 m_e c/4\pi\hbar$ is the Rydberg constant). More than ten years ago, comparisons of rates between clocks based on hyperfine transitions in alkali atoms with different atomic number Z (H-maser and Hg^+ clocks) over 140 days yielded a bound: $|\dot{\alpha}/\alpha| \leq 3.7 \times 10^{-14}\mathrm{yr}^{-1}$ 56).

Recently, by comparing a $^{199}Hg^+$ optical clock (($^2S_{1/2}F = 0$) - ($^2D_{5/2}F = 2, m_F = 0$) electric-quadrupole transition at 282 nm) with a ^{133}Cs clock over 2 years, a much severer upper bound has been obtained: $|\dot{\alpha}/\alpha| \leq 1.2 \times 10^{-15}\mathrm{yr}^{-1}$ 57). The electric-quadrupole transition of $^{199}Hg^+$ is expressed as $R_\infty F_{\mathrm{Hg}}(\alpha)$, where $F_{\mathrm{Hg}}(\alpha)$ is a dimensionless function of α. Most recent measurement over 6 years gives $|\dot{\alpha}/\alpha| \leq 1.3 \times 10^{-16}\mathrm{yr}^{-1}$ 62) for $^{199}Hg^+$. Moreover, the comparison of the hyperfine frequencies of ^{133}Cs and ^{87}Rb atoms over nearly 5 years yields $\dot{\alpha}/\alpha = (0.045 \pm 1.6) \times 10^{-15}\mathrm{yr}^{-1}$ 58). The comparison of the absolute 1S-2S transition in atomic hydrogen to the ground state of cesium combined with the results of 57), 58) yields a constraint: $\dot{\alpha}/\alpha = (-0.9 \pm 2.9) \times 10^{-15}\mathrm{yr}^{-1}$ 59). However, hyperfine frequencies are sensitive not only to α but also to a variation of the nuclear magnetic moment. Moreover, since a microwave distorts atoms, the improvements in microwave cesium clocks beyond 10^{-16} are unlikely. With these motivations, recently, an optical electric quadrupole transition frequency at 436 nm in $^{171}Yb^+$ has been measured with a cesium atomic clock at two times separated by 2.8 years 60). Combined with the data with those for optical transition frequencies in $^{199}Hg^+$ from 57) and in hydrogen from 59) gives $\dot{\alpha}/\alpha = (-0.3 \pm 2.0) \times 10^{-15}\mathrm{yr}^{-1}$ 60). Comparisons of Hg^+ clocks 62) with Yb^+ and H yield $\dot{\alpha}/\alpha = (-0.55 \pm 0.95) \times 10^{-15}\mathrm{yr}^{-1}$ 62). Also, comparisons of optical Sr clocks 63) with Hg^+ 62), Yb^+ 61), and H 59) gives $\dot{\alpha}/\alpha = (-3.3 \pm 3.0) \times 10^{-16}\mathrm{yr}^{-1}$ 63). Recently, two optical clocks using Al^+ (($^1S_0$) - ($^3P_0$) clock transition at 267 nm) 64) and Hg^+ are compared directly without a cesium atomic clock 65). The transition frequency depends both on the Rydberg constant and on α and can be expressed as $R_\infty F_{\mathrm{Al}}(\alpha)$. From the ratio of the two transition frequencies, $\dot{\alpha}/\alpha = (-1.6 \pm 2.3) \times 10^{-17}\mathrm{yr}^{-1}$

is obtained 65), being independent of the assumptions on the constancy of other constants. The frequency uncertainties of the optical clocks are currently less than 2.3×10^{-17}. The accuracy could soon compete with the gravitational redshifts due to the difference in the heights of the clocks ($g\Delta h/c^2 \simeq 10^{-18}$ for the height difference $\Delta h = 1$cm) so that the optical clocks could be used to map the gravitational potential of the earth and to test gravitational physics 65), 66).

More recently, following the proposal of 67), it is demonstrated that, instead of comparing atomic-clock of different atomic number, the difference of the electronic energies of the opposite-parity levels in two isotopes of the same atomic dysprosium (Dy) can be monitored directly using a radio-frequency electric-dipole transition between them 68). Eight months measurements of the 3.1-MHz transition in ^{163}Dy and the 235-MHz transition in ^{162}Dy show that the frequency variation is 9.0 ± 6.7Hz/yr, -0.6 ± 6.5 Hz/yr. respectively, which corresponds to $\dot{\alpha}/\alpha = (-5.0 \pm 3.7) \times 10^{-15}\mathrm{yr}^{-1}$ for the 3.1-MHz transition and $\dot{\alpha}/\alpha = (-0.3 \pm 3.6) \times 10^{-15}\mathrm{yr}^{-1}$ for the 235-MHz transition. The difference frequency gives finally $\dot{\alpha}/\alpha = (-2.7 \pm 2.6) \times 10^{-15}\mathrm{yr}^{-1}$ 68). A unique aspect of this measurement is that the interpretation does not require comparison with different measurements to eliminate dependence on other constants. Current systematic uncertainties are at 1 Hz-level, but mHz-level sensitivity ($|\dot{\alpha}/\alpha| \sim 10^{-18}\mathrm{yr}^{-1}$) may be feasible with this method.

2.4. *Cosmology and $\dot{\alpha}$: Big Bang Nucleosynthesis and Cosmic Microwave Background*

2.4.1. Big Bang Nucleosynthesis.

The process of the Big Bang nucleosynthesis proceeds as follows. When the temperature of the universe is greater than 1MeV, protons and neutrons are interchanged by the weak interaction. The neutron-to-proton number ratio (n/p) is given by the equilibrium condition:

$$(n/p) = \exp(-Q/T), \tag{2·10}$$

where $Q = 1.29$MeV is the mass difference between neutron and proton. The equilibrium is violated when the expansion rate of the universe $H \simeq \sqrt{G}T^2$ becomes faster than the reaction rate of the weak interaction $n\sigma v \simeq G_F^2 T^5$, where G_F is the Fermi constant. The balance of these two rates determines the freeze-out temperature,

$$T_f \simeq G_F^{-2/3} G^{1/6} \simeq 1\mathrm{MeV}. \tag{2·11}$$

For the temperature below 1MeV, the number of neutrons decreases only due to the natural decay with the life time being 15 minutes. Deuterons, ^{3}H$_e$s and finally ^{4}H$_e$s are produced by nuclear interactions of protons and neutrons. All the neutrons are incorporated into ^{4}H$_e$ and the abundance of ^{4}H$_e$, Y_p, is given by $Y_p = 2(n/p)/[1 + (n/p)]$. Changes in Y_p are induced by changes in T_f and Q. However, it is found that Y_p is most sensitive to changes in Q 69). The α dependence of Q can be written as 70)–72)

$$Q \simeq 1.29 - 0.76 \times \Delta\alpha/\alpha \ \ \mathrm{MeV}, \tag{2·12}$$

and change in Y_p is related to the change in α as

$$\frac{\Delta Y}{Y} \simeq -\frac{\Delta Q}{Q} \simeq 0.6\frac{\Delta\alpha}{\alpha}. \tag{2·13}$$

Comparing with the observed $Y_p(Y_p = 0.249 \pm 0.009)$73), a constraint on $\Delta\alpha/\alpha$ is obtained: $|\Delta\alpha/\alpha| \leq 6 \times 10^{-2}$ 74). A similar analysis yields a bound on ΔQ: $-4 \times 10^{-2} \leq \Delta Q/Q \leq 2.7 \times 10^{-2}$ 75), which can be translated into a bound on $\Delta\alpha$ via Eq. (2·13) as, $-4.5 \times 10^{-2} \leq \Delta\alpha/\alpha \leq 6.7 \times 10^{-2}$.

2.4.2. Cosmic Microwave Background.

Changing α changes the Thomson scattering cross section, $\sigma_T = 8\pi\alpha^2/3m_e^2$ and also changes the differential optical depth $\dot{\tau}$ of photons due to Thomson scattering through $\dot{\tau} = x_e n_p \sigma_T$ where x_e is the ionization fraction and n_p is the number density of electrons. From the Saha equation, the equilibrium ionization fraction x_e^{EQ} is proportional to $(m_e/T)^{3/2}\exp(-\alpha^2 m_e/2T)$. Therefore, changing α alters the ionization history of the universe and hence affects the spectrum of cosmic microwave background fluctuations.

The last scattering surface is defined by the peak of the visibility function, $g(z) = e^{-\tau(z)}d\tau/dz$, which measures the differential probability that a photon last scattered at redshift z. As explained in 76), increasing α affects the visibility function $g(z)$: it increases the redshift of the last scattering surface and decreases the thickness of the last scattering surface. This is because the equilibrium ionization fraction x_e^{EQ}, which is exponentially sensitive to α, is shifted to higher redshift (the effect of increase of $\dot{\tau}$ due to the increase of σ_T is minor) and because x_e more closely tracks x_e^{EQ} for larger α.

An increase in α changes the spectrum of CMB fluctuations: the peak positions in the spectrum shift to higher values of ℓ (that is, a smaller angle) and the values of C_ℓ increase 76). The former effect is due to the increase of the redshift of the last scattering surface, while the latter is due to a larger early integrated Sachs-Wolfe effect because of an earlier recombination. Beyond the first peak, the diffusion damping of CMB fluctuation due to the thickness of the last scattering surface becomes important 76), 77). The diffusion damping is caused by the random walk of CMB photons and hence the diffusion length λ_D is given by $\lambda_D \simeq 1/\sqrt{H\dot{\tau}}$. The damping factor of CMB fluctuations is estimated as $\sim \exp(-\lambda_D^2/\lambda^2)$ for a given wavelength λ of the fluctuations. A large α shortens the diffusion length λ_D and hence weakens the effect of diffusion damping and makes the values of C_ℓ increase.

The analysis of the first-year observations from the WMAP(Wilkinson Microwave Anisotropy Probe) satellite 14) gives $-0.06 < \Delta\alpha/\alpha < 0.01$ at 2 σ 78). The five-year WMAP data combined with the CMB data sets by ACBAR, QUAD, BICEP, BOOMERanG and CBI and with the recent measurement of the Hubble constant by HST 79) improves the accuracy: $-0.011 < \Delta\alpha/\alpha < 0.015$ at 2 σ 80). A recent analysis of the seven-year WMAP data combined with the matter power spectrum of Sloan Digital Sky Survey LRG yields $\Delta\alpha/\alpha = -0.014 \pm 0.014$ at 2 σ 81).

2.4.3. Constraints at $30 < z < 1000$ and $z < 1$.

Several probes of variations in α after the epoch of last scatter have been proposed: 21 cm absorption of CMB 82) and peak luminosity of type Ia supernovae (SNIa) 83). The former probes the variation for redshifts in the range $30 < z < 1000$, while the latter at $z < 1$.

After recombination ($z \sim 1000$)and before reionization ($z \sim 30$), hydrogen atoms are in ground state which is split into a singlet and a triplet state due to hyperfine splitting. The absorption of CMB at 21 cm hyperfine transition of the neutral atomic hydrogen is very sensitive to the variations in α. The Einstein A coefficient of the spontaneous emission of the 21 cm transition is proportional to α^{13} and the brightness temperature signal of CMB at 21 cm T_b is proportional to α^5 82). Future radio telescopes may give a constraint on $\Delta\alpha$ of 1% 82).

A Type Ia supernova is considered to be a good standard candle, because its peak luminosity correlates with the rate of decline of the magnitude. Observations of Type Ia supernovae have been used to constrain cosmological parameters. The homogeneity of the peak luminosity is essentially due to the homogeneity of the progenitor mass, and this is primarily determined by the Chandrasekhar mass, which is proportional to $G^{-3/2}$. The peak luminosity also depends on the diffusion time of photons, which depends on α through the opacity. A decrease in opacity reduces the diffusion time, allowing trapped radiation to escape more rapidly, leading in turn to an increase in the luminosity. Decreasing α causes the opacity to decrease, which allows photons to escape more rapidly, thereby leading to an increase in the luminosity. Thus a smaller (larger) value of α would make supernovae brighter (fainter). The change in the absolute magnitude $\Delta\mathcal{M}$ at the peak luminosity is related to the variation in α as $\Delta\mathcal{M} \simeq (\Delta\alpha/\alpha)^{-1}$ 83). Future experiments to observe distant SNIa like SNAP would reduce systematic errors to a magnitude of 0.02 mag, which corresponds to $\Delta\alpha/\alpha < 2 \times 10^{-2}$. This bound is significantly larger than the current bound by QSO for redshifts in the range $0.5 < z < 2$: $\Delta\alpha/\alpha \lesssim 10^{-5}$.

§3. *G*

In this section, we review the experimental constraints on time variation of the gravitational constant. For more detailed earlier review see 106). The results are summarized in Table III.

3.1. *Viking Radar-Ranging to Mars, Lunar-Laser-Ranging and $\dot{G}$*

If we write the effective gravitational constant G as $G = G_0 + \dot{G}_0(t - t_0)$, the effect of changing G is readily seen through the change in the equation of motion:

$$\frac{d^2\mathbf{x}}{dt^2} = -\frac{GM\mathbf{x}}{r^3} = -\frac{G_0 M\mathbf{x}}{r^3} - \frac{\dot{G}_0}{G_0}\frac{G_0 M}{r}\frac{\mathbf{x}(t-t_0)}{r^2}. \tag{3·1}$$

Thus time variation of G induces an acceleration term of secular type in addition to the usual Newtonian and relativistic ones, which would affect the motion of bodies, such as planets and binary pulsar.

A relative distance between the Earth and Mars was accurately measured by

taking thousands of range measurements between tracking stations of the Deep Space Network and Viking launders on Mars. From a least-squares fit of the parameters of the solar system model to the data taken from various range measurements including those by Viking landers to Mars (from July 1976 to July 1982), a bound on $\dot{G}$ is obtained: $\dot{G}/G = (2 \pm 4) \times 10^{-12}\mathrm{yr}^{-1}$ 84).

Similarly, Lunar-Laser-Ranging measurements have been used to accurately determine parameters of the solar system, in particular the Earth-Moon separation. From the analysis of the data from 1969 to 1990, a bound is obtained: $\dot{G}/G = (0.1 \pm 10.4) \times 10^{-12}\mathrm{yr}^{-1}$ 85); while from the data from 1970 to 1994, $\dot{G}/G = (1 \pm 8) \times 10^{-12}\mathrm{yr}^{-1}$ 86). Recent analyses using the data up to April 2004 results in $\dot{G}/G = (4 \pm 9) \times 10^{-13}\mathrm{yr}^{-1}$ 87). The uncertainty for $\dot{G}/G$ is improving rapidly since the sensitivity for the observations depends on the square of the time span.

	redshift	$\Delta G/G$	$\dot{G}/G(\mathrm{yr}^{-1})$
Viking Lander Ranging[84)]	0		$(2 \pm 4) \times 10^{-12}$
Lunar Laser Ranging[87)]	0		$(4 \pm 9) \times 10^{-13}$
Double Neutron Star Binary[89)]	0		$(1.10 \pm 1.07) \times 10^{-11}$
Pulsar-White Dwarf Binary[92)]	0		$(-5 \pm 18) \times 10^{-12}$
Helioseismology[95)]	0		$< 1.6 \times 10^{-12}$
White Dwarf Luminosity Function[97)]	0		$< 1.8 \times 10^{-12}$
Neutron Star Mass[98)]	$0 - 3 \sim 4$		$(-0.6 \pm 2.0) \times 10^{-12}$
Gravochemical Heating[99)]	0		$< 4 \times 10^{-10}$
BBN[101)]	10^{10}	$-0.3 \sim 0.4$	$(-2.9 \sim 2.2) \times 10^{-11}$
BBN+CMB[102)]	10^{10}	$-0.15 \sim 0.21$	$(-1.5 \sim 1.1) \times 10^{-11}$
BBN+CMB[74)]	10^{10}	$-0.10 \sim 0.13$	$(-0.95 \sim 0.73) \times 10^{-11}$
CMB[104)]	10^{3}	< 0.05	$< 3.6 \times 10^{-12}$

Table III. Summary of the experimental bounds on time variation of the gravitational constant. $\Delta G/G \equiv (G_{\mathrm{then}} - G_{\mathrm{now}})/G_{\mathrm{now}}$.

3.2. *Binary Pulsar and $\dot{G}$*

The timing of the orbital dynamics of binary pulsars provides a new test of time variation of G. To the Newtonian order, the orbital period of a two-body system is given by

$$P_b = 2\pi \left(\frac{a^3}{Gm}\right)^{1/2} = \frac{2\pi\ell^3}{G^2m^2(1-e^2)^{3/2}}, \tag{3·2}$$

where a is the semi-major axis, $\ell = r^2\dot{\phi}$ is the angular momentum per unit mass, m is a Newtonian-order mass parameter, and e is the orbital eccentricity. This yields the orbital-period evolution rate

$$\frac{\dot{P}_b}{P_b} = -2\frac{\dot{G}}{G} + 3\frac{\dot{\ell}}{\ell} - 2\frac{\dot{m}}{m}. \tag{3·3}$$

Damour, Gibbons and Taylor showed that the appropriate phenomenological limit on $\dot{G}$ is obtained by

$$\frac{\dot{G}}{G} = -\frac{\delta \dot{P}_b}{2P_b}, \tag{3·4}$$

where $\delta \dot{P}_b$ represents whatever part of the observed orbital period derivative that is not otherwise explained 88). From the timing of the binary pulsar PSR 1913+16, a bound is obtained: $\dot{G}/G = (1.0 \pm 2.3) \times 10^{-11}\mathrm{yr}^{-1}$ 88) (see also 89)) However, only for the orbits of bodies which have negligible gravitational self-energies, the simplifications can be made that $\dot{P}_b/P_b$ is dominated by $-2\dot{G}/G$ term. When the effect of the variation in the gravitational binding energy induced by a change in G is taken into account, the above bound is somewhat weakened depending on the equation of state 90). This may not be concern to neutron star - white dwarf binaries such as PSR B1855+09 ($\dot{G}/G = (-9 \pm 18) \times 10^{-12}\mathrm{yr}^{-1}$) 91) and J0437-4715 ($\dot{G}/G = (-5 \pm 18) \times 10^{-12}\mathrm{yr}^{-1}$) 92).

3.3. *Stars and $\dot{G}$*

Since gravity plays an important role in the structure and evolution of a star, a star can be a good probe of time variation of G. It can be shown that the luminosity of a star is roughly proportional to G^7 if free-free transition dominates the opacity 93). Increasing G is effectively the same, via the Poisson equation, as increasing the mass or average density of a star, which increases its average mean molecular weight and thus increases the luminosity of a star. and decrease its lifetime. Since a more luminous star burns more hydrogen, the depth of convection zone is affected which is determined directly from observations of solar p-mode (acoustic wave) spectra 94). Helioseismology enables us to probe the structure of the solar interior. Comparing the p-mode oscillation spectra of varying-G solar models with the solar p-mode frequency observations, a tighter bound on $\dot{G}$ is obtained: $|\dot{G}/G| \leq 1.6 \times 10^{-12}\mathrm{yr}^{-1}$ 95).

The balance between the Fermi degeneracy pressure of a cold electron gas and the gravitational force determines the famous Chandrasekhar mass

$$M_{Ch} \simeq G^{-3/2} m_p^{-2}, \tag{3·5}$$

where m_p is the proton mass, which is the upper bound of the masses of white dwarfs. White dwarfs are long-lived objects ($\sim$ 10 Gyr) and their inner cores are almost degenerate, hence even small variations of G can affect their structure and evolution. Moreover, white dwarfs do not have nuclear energy sources and their energy is of gravitational and thermal origin. The cooling process of white dwarfs is now well understood, including the energy release due to ^{22}Ne sedimentation in the liquid phase and due to C/O phase separation on crystallization in the core 96). The decrease in G (larger G in the past) accelerates the cooling of white dwarfs. By comparing the white dwarf luminosity function measured in the open cluster NGC 6791 with the simulated luminosity function, using the observed distance modulus to break the degeneracy between the age of the cluster and the effect of $\dot{G}$, a tighter bound on $\dot{G}$ is obtained; $\dot{G}/G > -1.8 \times 10^{-12}$ 97).

M_{Ch} sets the mass scale for the late evolutionary stage of massive stars, including the formation of neutron stars in core collapse of supernovae, and it is thus expected that the average neutron mass is given by the Chandrasekhar mass. Measurements of neutron star masses and ages over $0 < z < 3 \sim 4$ yield a bound, $\dot{G}/G = (-0.6 \pm 2.0) \times 10^{-12}\mathrm{yr}^{-1}$ 98).

Recently, a new method for constraining $\dot{G}$ is proposed using the surface temperatures of neutron stars (dubbed "gravochemical heating")99). An increase (or decrease) in G induces the compression (or expansion) of the star. Since the chemical potentials depend on the density, the system interior to the star departs from the beta equilibrium state, which increases the chemical reaction rates so as to reach a new equilibrium state, dissipating energy as internal heating and neutrino emission. Comparing the ultrainfrared observation of the surface temperature of the millisecond pulsar (PSR J0437-4715), upper limits on $\dot{G}$ are obtained: $|\dot{G}/G| < 2\times10^{-10}\mathrm{yr}^{-1}$ if direct Urca reaction operating in the neutron star core is allowed, while $|\dot{G}/G| < 4 \times 10^{-10}\mathrm{yr}^{-1}$ if only modified Urca reactions are considered 99).

3.4. *Cosmology and $\dot{G}$: Big-Bang Nucleosynthesis and Cosmic Microwave Background*

3.4.1. Big Bang Nucleosynthesis.

The effect of changing G on the primordial light abundances (especially $^4\mathrm{H_e}$) is already seen in Eq.(2·10) and Eq.(2·11): an increase in G increases the expansion rate of the universe, which shifts the freeze-out to an earlier epoch and results in a higher abundance of $^4\mathrm{H_e}$. In terms of the "speed-up factor"(the ratio of the Hubble parameter to that in the Standard Big Bang Nucleosynthesis), $\xi \equiv H/H_{SBBN}$, Y_p is well fitted by 100)

$$Y_p \simeq 0.244 + 0.074(\xi^2 - 1). \tag{3·6}$$

If Y_p was between 0.22 and 0.25, then $-0.32 < \Delta G/G < 0.08$, which corresponds to $\dot{G}/G = (-0.55 \sim 2.2) \times 10^{-11}\mathrm{yr}^{-1}$. A similar (more conservative) bound was obtained in 101) : $-0.3 < \Delta G/G < 0.4$. Combining the determination by WMAP of $\Omega_b h^2$ and recent measurements of primordial deuterium abundance (but without Helium and Lithium abundance), a slightly tighter constraint is obtained 102) : $-0.15 < \Delta G/G < 0.21$. By combining WMAP value of $\Omega_b h^2$ and recent results of the reanalysis of helium abundance 73), similar bound has been obtained: $-0.10 < \Delta G/G < 0.13$ 74). It should be noted that the analysis by WMAP team assumed the Einstein gravity and hence the effect of changing G is not included. Hence, these analyses are not consistent and should be made in the context of scalar-tensor gravity (or its variants) consistently.

3.4.2. Cosmic Microwave Background.

Changing G changes the Hubble parameter and hence changes the size of horizon: $H^{-1} \propto G^{-1/2}$, which results in the change of both the location and the amplitude of acoustic peaks through the projection effects and the diffusion damping scale 103). For example, an increase in G shifts the peak positions in the spectrum toward higher values of ℓ. A larger G makes the diffusion length $\lambda_D \simeq 1/\sqrt{H\dot{\tau}}$ shorter and thus weakens the diffusion damping at the peak positions because the peak positions also

depend on H^{-1} ($\lambda \propto H^{-1}$) and hence the damping factor $\exp(-\lambda_D^2/\lambda^2)$ decreases less.

Recently, anisotropies in the cosmic microwave background have been measured up to $\ell < 800$ by WMAP satellite 14). From the analysis of the WMAP data within the context varying G model, the variation of the gravitational constant at the recombination epoch is constrained as 104) : $\Delta G/G < 0.05$.

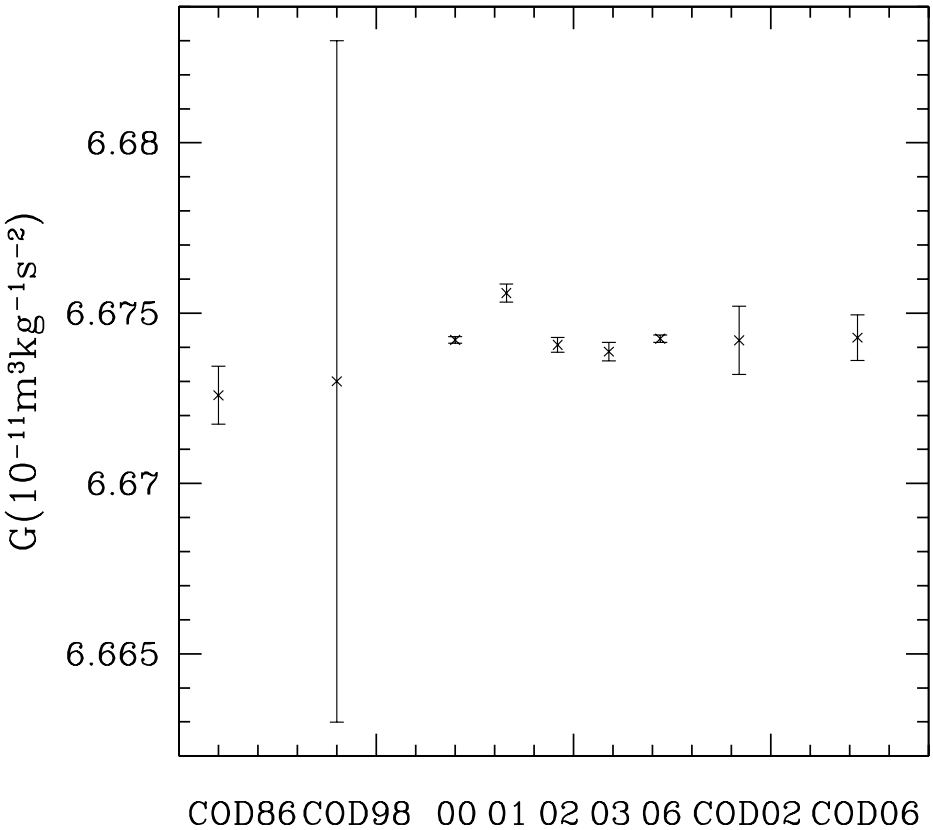

Fig. 2. Experimental results on measurements of G.

3.5. *Measuring G_0: Recent Developments*

In 1798, Cavendish carried out experiments to measure G_0 by using a torsion balance apparatus (proposed and constructed by John Michell), which has become known as the Cavendish Experiment 105). The basic method is still used in measuring G_0.

The torsion balance consists of a dumbbell suspended from the middle by a thin fiber. The dumbbell consists of two small masses (m) fastened to a thin rod of

length 2ℓ. When a large pair of masses (M) are brought into proximity to the smaller masses, the dumbbell rotates by an angle φ_0 and comes to a halt. From the balance between the torsion of the fiber (the torsion coefficient D) and the torque due to the gravity force between m and M (the distance r), we have $D\varphi_0 = 2G_0 Mm\ell/r^2$. When the large masses are removed from the set up, the dumbbell begins to oscillate because of the restoring force of the fiber. The period of oscillation T is given by $T = 2\pi\sqrt{I/D}$ where $I(= 2m\ell^2)$ is the moment of inertia of the dumbbell. Eliminating D, G_0 is thus determined by $G = 4\pi^2 r^2 \varphi_0 \ell/MT^2$.

No laboratory measurements of $\dot{G}/G$ has been performed recently (see 106) for older laboratory experiments). This is mainly because the measurements of the present gravitational constant G_0 itself suffer from systematic uncertainties and have not been performed with good precision. For example, due to the uncertainties associated with the frequency dependence of the torsion coefficient of fibers, the recommended value of G_0 by CODATA (Committee on Data for Science and Technology) became worsened from $G = (6.67259 \pm 8.5 \times 10^{-4}) \times 10^{-11}\mathrm{m}^3\mathrm{kg}^{-1}\mathrm{s}^{-2}$ in 1986 to $(6.673 \pm 1.0 \times 10^{-2}) \times 10^{-11}$ in 1998 107).

Gundlach and Merkowitz measured G_0 with a torsion-balance experiment in which string-twisting bias was carefully eliminated 108). The result was a value of $G_0 = (6.674215 \pm 0.000092) \times 10^{-11}\mathrm{m}^3\mathrm{kg}^{-1}\mathrm{s}^{-2}$. Recently, however, the measurement of G with a torsion-strip balance resulted in $G_0 = (6.67559 \pm 0.00027) \times 10^{-11}\mathrm{m}^3\mathrm{kg}^{-1}\mathrm{s}^{-2}$, which is 2 parts in 10^4 higher than the result of Gundlach and Merkowitz 109). Probably the difference is still due to systematic errors hidden in one or both of the measurements. On the other hand, recent beam balance measurement ($G_0 = (6.67407 \pm 0.00022) \times 10^{-11}\mathrm{m}^3\mathrm{kg}^{-1}\mathrm{s}^{-2}$) 110) and torsion balance measurement ($G_0 = (6.67387 \pm 0.00027) \times 10^{-11}\mathrm{m}^3\mathrm{kg}^{-1}\mathrm{s}^{-2}$) 111) of G are consistent with the result by Gundlach and Merkowitz. A new measurement of G was made using a beam balance 112). The measured value, $G_0 = (6.674252 \pm 0.000109) \times 10^{-11}\mathrm{m}^3\mathrm{kg}^{-1}\mathrm{s}^{-2}$, is consistent with that by Gundlach and Merkowitz. *) The recommended value of G by CODATA is being improved: $G = (6.6742 \pm 1.0 \times 10^{-3}) \times 10^{-11}\mathrm{m}^3\mathrm{kg}^{-1}\mathrm{s}^{-2}$ for CODATA 2002 115), while $G = (6.67428 \pm 6.7 \times 10^{-4}) \times 10^{-11}\mathrm{m}^3\mathrm{kg}^{-1}\mathrm{s}^{-2}$ for CODATA 2006 116). The values of G as a function of the year of measurements are shown in Fig. 2.

Moreover, conceptually different experiments of measuring G using a gravity gradiometer based on cold-atom interferometry were performed 117), 118). Freely falling samples of laser-cooled atoms are used in a gravity gradiometer to probe the field generated by nearby source masses. A measured value of G is, $G = (6.667 \pm 0.011 \pm 0.003) \times 10^{-11}\mathrm{m}^3\mathrm{kg}^{-1}\mathrm{s}^{-2}$ 118). It may be possible to push the measurement accuracy below 10^{-4}.

*) However, two recent determinations of G, one by comparing the time it took for a torsion pendulum to swing past masses placed at varying distances from it 113) and another by using a laser interferometer to measure the displacement of pendulum bobs by various masses 114), give values significantly deviated from the value by Gundlach and Merkowitz: $G_0 = (6.67349 \pm 0.00018) \times 10^{-11}\mathrm{m}^3\mathrm{kg}^{-1}\mathrm{s}^{-2}$ 113) and $G_0 = (6.67259 \pm 0.00085) \times 10^{-11}\mathrm{m}^3\mathrm{kg}^{-1}\mathrm{s}^{-2}$ 114). The source of the inconsistency is currently unknown, and these new values may make the next recommended value of G by CODATA decrease and make the uncertainty larger.

As the accuracy of the measurements improves, it may be possible to place a bound on a present-day variation of G. Although the current accuracy of G is more than 6 digits worse than the solar system experiments or cosmological constraints to place a constraint on the present-day $\dot{G}$, the situation will be changed after a century since the accuracy improves by one digit during these ten years. It is important to pursue laboratory measurements of $\dot{G}/G$ since they are repeatable and hence are complementary to astrophysical and geophysical constraints.

§4. Proton-Electron Mass Ratio

In this section, we briefly mention the experimental constraints on the variation of the electron-proton mass ratio, $\mu = m_p/m_e$. The results are summarized in Table IV.

	redshift	$\Delta\mu/\mu$	$\dot{\mu}/\mu(\mathrm{yr}^{-1})$
Atomic Clock(Mg)[54]	0		$(2.5 \pm 2.3) \times 10^{-13}$
Atomic Clock(Hg)[57]	0		$\pm 7.0 \times 10^{-15}$
Atomic Clock(Sr)[63]	0		$(-1.6 \pm 1.7) \times 10^{-15}$
Molecular Clock(SF_6)[143]	0		$(-3.8 \pm 5.6) \times 10^{-14}$
HI[31]	2.811	$(-0.8 \sim 3.1) \times 10^{-5}$	$(0.7 \sim 2.7) \times 10^{-15}$
H_2[31]	1.7764	$(-0.7 \sim 0.6) \times 10^{-5}$	$(0.7 \sim 0.6) \times 10^{-15}$
HI/H_2[121]	$0.24 - 2.04$	$(-1.29 \pm 1.01) \times 10^{-5}$	
H_2[122]	2.81	$(8.3^{+6.6}_{-5.0}) \times 10^{-5}$	$(-7.3^{+4.5}_{-5.8}) \times 10^{-15}$
H_2[123]	2.3377, 3.0249	$(5.7 \pm 3.8) \times 10^{-5}$	$(-5.1 \pm 3.4) \times 10^{-15}$
H_2[124]	2.3377, 2.8108, 3.0249	$(-0.5 \pm 3.6) \times 10^{-5}$	$0.4 \pm 3.2) \times 10^{-15}$
H_2[125]	2.5947, 3.0249	$(1.65 \pm 0.74) \times 10^{-5}$	$(-1.46 \pm 0.65) \times 10^{-15}$
H_2[126]	2.5947, 3.0249	$(2.44 \pm 0.59) \times 10^{-5}$	$(-2.16 \pm 0.52) \times 10^{-15}$
H_2[127]	2.595, 3.025, 2.811	$(2.6 \pm 3.0) \times 10^{-6}$	$(-2.3 \pm 2.7) \times 10^{-16}$
H_2/HD[128]	2.059	$(5.6 \pm 5.5) \times 10^{-6}$	$(-5.3 \pm 5.2) \times 10^{-16}$
H_2/HD[129]	2.059	$(8.5 \pm 3.6) \times 10^{-6}$	$(-8.0 \pm 3.4) \times 10^{-16}$
H_2/HD[130]	2.811	$(0.3 \pm 3.2) \times 10^{-6}$	$(-0.3 \pm 2.8) \times 10^{-16}$
OH/HCO^+/HI[131]	0.684	$(0.27 \pm 1.6) \times 10^{-3}$	$(-0.44 \pm 2.6) \times 10^{-13}$
OH[135]	0.247	$(-6.2 \pm 2.4) \times 10^{-6}$	$(2.1 \pm 0.8) \times 10^{-15}$
OH/HI[136]	0.765, 0.685	$\pm 1.4 \times 10^{-5}$	$< 2.2 \times 10^{-15}$
NH_3/CO,HCO^+,HCN[137]	0.68466	$(0.6 \pm 1.9) \times 10^{-6}$	$(-0.9 \pm 3.0) \times 10^{-16}$
NH_3/HCO^+,HCN[138]	0.68466	$(0.74 \pm 0.47) \times 10^{-6}$	$(-1.2 \pm 0.74) \times 10^{-16}$
NH_3, HC_3N[139]	0.89	$(0.08 \pm 0.47) \times 10^{-6}$	$(-0.11 \pm 0.64) \times 10^{-16}$

Table IV. Summary of the experimental bounds on time variation of the mass ratio of electron and proton, $\mu = m_p/m_e$. $\Delta\mu/\mu \equiv (\mu_{\rm then} - \mu_{\rm now})/\mu_{\rm now}$.

4.1. *Molecular lines and μ*

Thompson noted the different dependence of the electronic, vibrational, and rotational energy levels on μ and first pointed out the possibility that the presence of cosmological evolution in μ can be tested by using observations of molecular hydrogen in quasar absorption systems 119). In the Born-Oppenheimer approximation, the

molecular hydrogen levels depend on m_p and can be written as

$$E = E_{elec} + \frac{E_{vib}}{\sqrt{\mu}} + \frac{E_{rot}}{\mu}. \tag{4·1}$$

Thus, the energy shift in any vibration-rotation transition j in the Lyman series has the form

$$\Delta E_j = a_{elec} + b_j/\sqrt{\mu} + c_j/\mu, \tag{4·2}$$

and the difference in energy between two transitions is

$$\Delta E_i - \Delta E_j \simeq b_{ij}/\sqrt{\mu} + c_{ij}/\mu. \tag{4·3}$$

Hence, to lowest order, a change in μ induces a change in $\Delta E_i - \Delta E_j$:

$$\frac{\delta\mu}{\mu} \simeq -2\frac{\delta(\Delta E_i - \Delta E_j)}{\Delta E_i - \Delta E_j} \simeq -\frac{\delta v}{c}\frac{2\Delta E_i}{\Delta E_i - \Delta E_j}, \tag{4·4}$$

where δv is the mean offset, compared to the laboratory value, of the energy difference between the two sets of lines, when that offset is represented as a velocity difference. Based on this method, Pagel first obtained a constraint, $|\dot{\mu}/\mu| < 5 \times 10^{-11}$ from the comparison of different redshifts determined by neutral hydrogen molecule and by heavy ion absorption lines 120). The ratio of the hyperfine 21 cm absorption transition of neutral hydrogen to an optical resonance transition is dependent on $g_p\mu\alpha^2$, where g_p is the proton gyromagnetic ratio. Comparing the measured redshifts of 21 cm and optical absorption a constraint on the change in μ is obtained at $z = 1.7764$ 31): $\Delta\mu/\mu = (-0.7 \pm 1.1) \times 10^{-5}$ assuming that α and g_p are constants (note the different definition of μ used there and we changed the 95% confidence limits given in 31) into 1σ ones). Various observational constraints obtained so far are summarized in Table IV.

Recent measurements of H_2 lines of Lyman and Werner bands toward the quasars Q0405-443 and Q0347-383 with VLT/UVES indicate a systematic shift of μ in the past, $\Delta\mu/\mu = (1.65 \pm 0.74) \times 10^{-5}$ 125), but the results depend on the laboratory wavelengths: the above value is for wavelengths derived from a direct determination using laser techniques, while $\Delta\mu/\mu = (3.05 \pm 0.75) \times 10^{-5}$ for those derived from energy level determination 125). In general, a measured i-th molecular line wavelength λ_i in an absorption system at redshift z_{abs} is given by 122)

$$\lambda_i = \lambda_i^0(1 + z_{abs})(1 + K_i\Delta\mu/\mu), \tag{4·5}$$

where λ_i^0 is the laboratory transition wavelength and $K_i = d\ln\lambda_i/d\ln\mu$ is the sensitivity coefficient. With an improved calculation of sensitivity coefficients K_i and new accurate laboratory spectroscopic measurements, the reanalysis of the data 125) strengthen the case for a larger μ in the past 126) : $\Delta\mu/\mu = (2.44 \pm 0.59) \times 10^{-5}$. However, it is pointed out that the techniques used to calibrate the wavelength scale of the Ultraviolet and Visual Echelle Spectrograph (UVES) on VLT produce calibration errors 49). Reanalysis of the spectra by using the improved wavelength calibration techniques and improved fitting procedures yields a constraint

on $\Delta\mu/\mu$ as $\Delta\mu/\mu = (2.6 \pm 3.0) \times 10^{-6}$, which is consistent with no variation at 1 σ 127). Recent observations of a number of hydrogen lines (H_2 and HD) in the spectrum of J2123-0050 with Keck/HIRES at $z = 2.059$ yield a strong constraint: $\Delta\mu/\mu = (5.6 \pm 5.5(\text{stat}) \pm 2.9(\text{sys})) \times 10^{-6}$ 128). The analysis of the spectrum of the same object observed with VLT/UVES gives a similar constraint: $\Delta\mu/\mu = (8.5 \pm 3.6(\text{stat}) \pm 2.2(\text{sys})) \times 10^{-6}$ 129). The analysis of a new spectrum of Q0528-250 with VLT/UVES yields $\Delta\mu/\mu = (0.3 \pm 3.2(\text{stat}) \pm 1.9(\text{sys})) \times 10^{-6}$ 130).

Recently, the method of using 18 cm OH lines has been proposed 131)–133) to avoid possible systematic errors from multiple species which may have systematic velocity offsets. The ground $^2\Pi_{3/2} J = 3/2$ rotation state of OH is split into two levels by Λ doubling and each of these Λ doubling states is further split into two hyperfine states. Transitions between these levels lead to four spectral lines with wavelength $\sim$ 18 cm. Transitions with $\Delta F = 0$ are called the main lines, with frequencies of 1665.4018 and 1667.3590 MHz, while transitions with $\Delta F = 1$ are called satellite lines, with frequencies of 1612.2310 and 1720.5299 MHz. Since the four OH lines arise from two very different physical processes, Λ-doubling and hyperfine splitting, the transition frequencies have different dependences on the fundamental constants, α and μ and the proton gyromagnetic ratio g_p. Therefore, measurements of these lines enables us to constrain variations in α and μ from a single species. The radio observations of two satellite lines at $z = 0.247$ yield $\Delta X/X = (2.2 \pm 3.8) \times 10^{-5}$ for $X = g_p(\mu\alpha^2)^{1.85}$ 134). Assuming that the variations of α and the proton gyromagnetic ratio are small, a change in μ is constrained as, $\Delta\mu/\mu = (1.2 \pm 2.0) \times 10^{-5}$ 134). Deep Westerbork Synthesis Radio Telescope and Arecibo Telescope observations of these satellite lines yield $\Delta X/X = (-1.18 \pm 0.46) \times 10^{-5}$, suggesting 2.6σ evidence for a change in X 135). The limiting cases, assuming that only α or μ changes, are $\Delta\alpha/\alpha = (-3.1 \pm 1.2) \times 10^{-6}$ and $\Delta\mu/\mu = (-6.2 \pm 2.4) \times 10^{-6}$ 135). All four 18 cm OH lines have recently been detected at $z = 0.765$ with low signal-to-noise ratio 136), which, when combined with HI 21 cm lines at $z = 0.685$, yields a constraint of $|\Delta\mu/\mu| < 1.4 \times 10^{-5}$ 136).

It is pointed out recently that the inversion transition frequencies of ammonia (NH_3) are significantly sensitive to the variation of μ 137). By comparing the inversion spectrum of NH_3 with rotational spectra of other molecules (CO,HCO^+,HCN) at $z = 0.6847$, a strong constraint is obtained: $\Delta\mu/\mu = (-0.6 \pm 1.9) \times 10^{-6}$ 137). More detailed comparison of the NH_3 inversion transitions with HCO^+ and HCN molecular rotational transitions, a stronger constraint is obtained: $\Delta\mu/\mu = (0.74 \pm 0.47(\text{stat}) \pm 0.76(\text{sys})) \times 10^{-6}$ and a 2σ constraint of $|\Delta\mu/\mu| < 1.8 \times 10^{-6}$ 138). Also, from the comparison of the NH_3 inversion transitions with HCO^+ and HC_3N molecular rotational transitions at $z = 0.89$, a similar bound is obtained: $\Delta\mu/\mu = (0.08 \pm 0.47) \times 10^{-6}$ and a 3σ constraint of $|\Delta\mu/\mu| < 1.4 \times 10^{-6}$ 139). Moreover, from the spectral observations of molecular cores in the disk of the Milky Way in molecular transitions of NH_3 and HC_3N at the Effelsberg radio telescopes, a statistically significant velocity offset $23 \pm 4_{\text{stat}} \pm 3_{\text{sys}}$m/s between the radial velocities NH_3 and HC_3N is found 140). When interpreted in terms of the local (spatial) variation of μ, this implies a tentative signal of $\Delta\mu/\mu = (-26 \pm 1_{\text{stat}} \pm 3_{\text{sys}}) \times 10^{-9}$ 140), where $\Delta\mu \equiv (\mu_{\text{MilkyWay}} - \mu_{\text{lab}})/\mu_{\text{lab}}$. However, since the number of sources is small

and a different velocity offset is observed at a different epoch of the observations, there may exist unaccounted for systematic effects.

Very recently, torsion-vibrational frequencies of methanol (CH_3OH) are found to be far more sensitive to the variation of μ 141). Using the published data of observing narrow emission lines of the methanol masers in the Milky Way, the local (spatial) variation of μ is constrained as $\Delta\mu/\mu = (-11 \pm 17) \times 10^{-9}$ 142).

4.2. *Laboratory Tests: Clock Comparison*

Laboratory limits on variations of μ are obtained by comparison of atomic clocks or molecular clocks 54),57),63) as explained in Sec. 2.3. Recently, from the comparison of the frequency of a rovibrational transition in SF_6 with the hyperfine transition in Cs, combined with 62) to break the degeneracy with variations of α and nuclear magnetic moment, a constraint of $\dot{\mu}/\mu = (-3.8 \pm 5.6) \times 10^{-14}\mathrm{yr}^{-1}$ is obtained 143).

§5. Λ or Dark Energy

Finally, we briefly comment on the potential variability of the cosmological constant (or dark energy) because in the runaway scenario of dilaton or moduli ϕ, $\dot{\alpha}/\alpha$ and $\dot{G}/G$ would close to $\dot{\phi}/\phi$ 6).

5.1. *Evidence for $\Lambda > 0$*

There are two arguments for the presence of dark energy. The first indirect evidence comes from the sum rule in cosmology:

$$\sum \Omega_i = 1, \tag{5·1}$$

where $\Omega_i \equiv 8\pi G\rho_i/3H_0^2$ is the density parameter of the i-th energy component, ρ_i. The density parameter of the curvature, Ω_K, is defined by $\Omega_K \equiv -k/a^2H_0^2$. Since the current observational data indicate that matter density is much less than the critical density $\Omega_M < 1$ and that the Universe is flat, we are led to conclude that the Universe is dominated by dark energy, $\Omega_{DE} = 1 - \Omega_M - \Omega_K > 0$.

The second evidence for dark energy is from the observational evidence for the accelerating universe 144) *):

$$\frac{\ddot{a}}{aH_0^2} = -\frac{1}{2}\left(\Omega_M(1+z)^3 + (1+3w)\Omega_{DE}(1+z)^{3(1+w)}\right) > 0, \tag{5·2}$$

where w is the equation of state of dark energy, $w \equiv p_{DE}/\rho_{DE}$. Since distance measurements to SNIa strongly indicate the Universe is currently accelerating, the Universe should be dominated by dark energy with negative pressure ($w < 0$). We note that another argument for negative pressure comes from the necessity of the epoch of the matter domination.

*) The Nobel prize in physics 2011 is awarded to S. Perlmutter, B. P. Schmidt and A. G. Riess for the discovery of the accelerating expansion of the Universe through observations of distant supernovae. Congratulations !

5.2. *Supernova and $\dot{\Lambda}$*

A current bound on the equation of state of dark energy from supernova data (580 supernovae) is $|w-1| \lesssim 0.07$ 145). Future observations of high redshift supernovae/galaxies/clusters/BAO would pin down the bound on w to $|w-1| \lesssim 0.01$. The extent of time variation of dark energy density is readily seen from the equation of motion:

$$\frac{\dot{\rho}_{DE}}{\rho_{DE}} = -3(1+w)H. \tag{5·3}$$

§6. Conclusion

A short account of the experimental constraints on the time variability of the constants of nature (α, G and μ) was given. Since there are some theoretical motivations for the time variability of the constants of nature and the implications of it are profound, it is worth examining whether the constancy of the constants of nature is just a very good approximation.

Let's keep shaking the pillars to make sure they're rigid! 146)

Acknowledgements

The author would like to acknowledge useful discussions with Yasunori Fujii, Naoto Kobayashi, Masahide Yamaguchi and Jun'ichi Yokoyama at varikous stages in completing this review. This work was supported in part by a Grant-in-Aid for Scientific Research (Nos.20540280 and 15740152) from the Japan Society for the Promotion of Science.

References

1) P.A.M. Dirac, Proc. Roy. Soc. (London) **A165** (1938) 198.
2) P.A.M. Dirac, Nature **139** (1937) 323.
3) G. Gamov, Phys. Rev. Lett. **19** (1967) 759.
4) T. Damour, arXiv:gr-qc/0210059.
5) M. Dine and N. Seiberg, Phys. Lett. **162B** (1985) 299; Phys. Rev. Lett. **55** (1985) 366; M. Dine, R. Rohm, N. Seiberg and E. Witten, Phys. Lett. **156B** (1985) 55.
6) E. Witten, in *Sources and Detection of Dark Matter and Dark Energy*, ed. D. Cline, (Springer, 2000), pp. 27-36.
7) T. Damour and A.M. Polyakov, Nucl. Phys. **B 423** (1994) 532.
8) W.J. Marciano, Phys. Rev. Lett. **52** (1984) 489.
9) K. Maeda, Mod. Phys. Lett. **A3** (1988) 243.
10) T. Chiba, *Constancy of the Constants of Nature*, In the Proceedings of Frontier of Cosmology and Gravitation, (YITP, Kyoto, April 25-27, 2001) (gr-qc/0110118).
11) F. J. Dyson, in *Aspects of Quantum Theory*, ed. A.Salam and E.P.Wigner, (Cambridge University Press, 1972), pp. 213-236.
12) J.D. Barrow and F.J. Tipler, *The Anthropic Cosmological Principle*, (Oxford University Press, 1986).
13) J. P. Uzan, Rev. Mod. Phys. **75** (2003) 403 (2003); Living Rev. Rel. **14** (2011) 2.
14) C.L. Bennett et al., Astrophys. J. Suppl. **148** (2003) 1.
15) A.I. Shlyakhter, Nature **264** (1976) 340.
16) T. Damour and F. Dyson, Nucl. Phys. **B 480** (1996) 37.
17) Y. Fujii, A. Iwamoto, T. Fukahori, T. Ohnuki, M. Nakagawa, H. Hikida, Y. Oura and P.

Möller, Nucl. Phys. **B 573** (2000) 377.
18) S.K. Lamoreaux and J.R. Torgerson, Phys. Rev. D **69** (2004) 121701.
19) Yu. V. Petrov, A. I. Nazarov, M. S. Onegin, V. Y. Petrov and E. G. Sakhnovsky, Phys. Rev. C **74** (2006) 064610.
20) C. R. Gould, E. I. Sharapov and S. K. Lamoreaux, Phys. Rev. C **74** (2006) 024607.
21) P.J. Peebles and R.H. Dicke, Phys. Rev. **128** (1962) 2006.
22) M.I. Smoliar et al. Science **271** (1996) 1099.
23) F.J. Dyson, Phys. Rev. Lett. **27** (1967) 1291.
24) P. Möller and J.R. Nix, Atomic Data and Nuclear Data Tables **39** (1988) 213.
25) M. Galeazzi, F. Fontanelli, F. Gatti and S. Vitale, Phys. Rev. C **63** (2000) 014302.
26) Y. Fujii and A. Iwamoto, Phys. Rev. Lett. **91** (2003) 261101.
27) K. A. Olive, M. Pospelov, Y. Z. Qian, G. Manhes, E. Vangioni-Flam, A. Coc and M. Casse, Phys. Rev. D **69**(2004) 027701.
28) C. Itzykson and J.-B. Zuber, *Quantum Field Theory* (McGraw-Hill, 1980).
29) J. N. Bahcall and E. E. Salpeter, Astrophys.J. **142** (1965) 1677; J. N. Bahcall, W.L.W. Sargent and M. Schmidt, Astrophys.J. **149** (1967) L11; J. N. Bahcall and M. Schmidt, Phys. Rev. Lett. **19** (1967) 1294.
30) A.M. Wolfe, R.L. Brown and M.S. Roberts, Phys. Rev. Lett. **26** (1976) 179.
31) L.L. Cowie and A. Songaila, Astrophys.J. **453** (1995) 596.
32) C.L. Carilli et al., Phys. Rev. Lett. **85** (2000) 5511.
33) J.K. Webb et al., Phys. Rev. Lett. **82** (1999) 884.
34) J.K. Webb et al., Phys. Rev. Lett. **87** (2001) 091301.
35) M.T. Murphy, J.K. Webb, V.V. Flambaum, J.X. Prochaska, A.M. Wolfe, Mon.Not.Roy.Astron.Soc. **327** (2001) 1237.
36) M.T. Murphy, J.K. Webb and V.V. Flambaum, Mon.Not.Roy.Astron.Soc. **345** (2003) 609.
37) M.T. Murphy, J.K. Webb and V.V. Flambaum, Lec. Not. Phys. **648** (2004) 131.
38) J. K. Webb, J. A. King, M. T. Murphy, V. V. Flambaum, R. F. Carswell and M. B. Bainbridge, arXiv:1008.3907 [astro-ph.CO].
39) R. Srianand, H. Chand, P. Petitjean and B. Aracil, Phys. Rev. Lett. **92** (2004) 121302; H. Chand, R. Srianand, P. Petitjean and B. Aracil, Astron. Astrophys. **417** (2004) 853.
40) H. Chand, P. Petitjean, R. Srianand and B. Aracil, Astron. Astrophys. **430** (2005) 47.
41) R. Quast, D. Reimers and S.A. Levshakov, Astron. Astrophys. **415** (2004) L7.
42) S.A. Levshakov, M. Centurion, P. Molaro, S. D'Odorico, Astron. Astrophys. **434** (2005) 827.
43) S.A. Levshakov, M. Centurion, P. Molaro, S.D'Odorico, D. Reimers, R. Quast, M. Pollmann, Astron. Astrophys. **449** (2006) 879.
44) P. Molaro, D. Reimers, I. I. Agafonova and S. A. Levshakov, Eur. Phys. J. ST **163**, 173 (2008).
45) H. Chand, R. Srianand, P. Petitjean, B. Aracil, R. Quast and D. Reimers, Astron. Astrophys. **451** (2006) 45.
46) Private communuication with Y. Fujii.
47) M.T. Murphy, J.K. Webb and V.V. Flambaum, Phys. Rev. Lett. **99** (2007) 239001; M.T. Murphy, J.K. Webb and V.V. Flambaum, Mon.Not.Roy.Astron.Soc. **384** (2008) 1053.
48) R. Srianand, H. Chand, P. Petitjean, B. Aracil, Phys. Rev. Lett. **99** (2007) 239002.
49) M.T. Murphy, P. Tzanavaris, J.K. Webb, C. Lovis, *Mon. Not. R. Astron. Soc.* **378** (2007) 221.
50) K. Griest et al., Astrophys. J. **708** (2010) 158.
51) M.T. Murphy, J.K. Webb, V.V. Flambaum, Mem.S.A.It. **80** (2009) 833.
52) "Testing the Possible Time Variation of Fine Structure Constant" (Subaru Telescope Semester S04A(Subaru Open Use Intensive Program)), P.I. Naoto Kobayashi; co-investigators, Takeshi Chiba, Masanori Iye, Yuzuru Yoshii, Chris Churchill, Takuji Tsujimoto, Naoshi Sugiyama, Yosuke Minowa.
53) J.P. Turneaure and S. Stein, in *Atomic Masses and Fundamental Constants Vol.5*, (Plenum, London, 1976), pp. 636-642.
54) A. Godone, C. Novero, P. Tavella and K. Rahimullah, Phys. Rev. Lett. **71** (1993) 2364.
55) Bureau International des Poids et Mesures, Sèvres, France, *Le Système International d'Unités (SI)*, 7th ed.

56) J.D. Prestage, R.L. Tjoelker and L. Maleki, Phys. Rev. Lett. **74** (1995) 3511.
57) S. Bize et al., Phys. Rev. Lett. **90** (2003) 150802.
58) H. Marion et al., Phys. Rev. Lett. **90** (2003) 150801.
59) M. Fischer et al., Phys. Rev. Lett. **92** (2004) 230802.
60) E. Peik et al., Phys. Rev. Lett. **93** (2004) 170801.
61) E. Peik et al., arXiv:/physics/0611088.
62) T.M. Fortier et al., Phys. Rev. Lett. **98** (2007) 070801.
63) S. Blatt et al., Phys. Rev. Lett. **100** (2008) 140801.
64) T. Rosenband et al., Phys. Rev. Lett. **98** (2007) 220801.
65) T. Rosenband et al., Science **319** (2008) 808.
66) C.W. Chou, D.B. Hume, T. Rosenband, D.J. Wineland, Science **329** (2010) 1630.
67) V.A. Dzuba, V.V. Flambaum and M.V. Marchenko, Phys. Rev. A **68** (2003) 022506.
68) A. Cingöz et al., Phys. Rev. Lett. **938** (2007) 040801.
69) E.W. Kolb, M.J. Perry and T.P. Walker, Phys. Rev. D **33** (1986) 869.
70) J. Gasser and H. Leutwyler, Phys. Rep. **87** (1982) 77.
71) V.V. Dixit and M. Sher, Phys. Rev. D **37** (1988) 1097.
72) B.A. Campbell and K.A. Olive, Phys. Lett. **B345** (1995) 429.
73) K.A. Olive and E.D. Skillman, Astrophys. J. **617** (2004) 29.
74) R.H. Cyburt, B.D. Fields, K.A. Olive, and E.D. Skillman Astropart. Phys. **23** (2005) 313.
75) A. Coc, N. J. Nunes, K. A. Olive, J. -P. Uzan, E. Vangioni, Phys. Rev. **D76** (2007) 023511.
76) S. Hannestad, Phys. Rev. D **60** (1999) 023515; M. Kaplinghat, R.J. Scherrer and M.S. Turner, Phys. Rev. D **60** (1999) 023516.
77) W. Hu and N. Sugiyama, Astrophys. J. **471** (1996) 542.
78) C.J.A. Martins et al., Phys. Lett. B **585** (2004) 29.
79) A. G. Riess *et al.*, Astrophys. J. Suppl. **183** (2009) 109.
80) E. Menegoni, S. Galli, J. G. Bartlett, C. J. A. Martins and A. Melchiorri, Phys. Rev. D **80** (2009) 087302.
81) S. J. Landau and C. G. Scoccola, Astron. Astrophys. **517** (2010) 62.
82) R. Khatri and B. D. Wandelt, Phys. Rev. Lett. **98** (2007) 111301.
83) T. Chiba and K. Kohri, Prog. Theor. Phys., **110** (2003) 195.
84) R.W. Hellings et al., Phys. Rev. Lett. **51** (1983) 1609.
85) J. Müller, M. Schneider, M. Soffel and H. Ruder, Astrophys.J. **382** (1991) L101.
86) J.G. Williams, X.X. Newhall and J.O. Dickey, Phys. Rev. D **53** (1996) 6730.
87) J.G. Williams, S.G. Turyshev and D.H. Boggs, Phys. Rev. Lett. **93** (2004) 261101.
88) T. Damour, G.W. Gibbons and J.H. Taylor, Phys. Rev. Lett. **61** (1988) 1152.
89) T. Damour and J.H. Taylor, Astrophys.J. **366** (1991) 501.
90) K. Nordtvedt, Phys. Rev. Lett. **65** (1990) 953.
91) V.M. Kaspi, J.H. Taylor and M.F. Ryba, Astrophys.J. **428** (1994) 713.
92) J.P.W. Verbiest et al., Astrophys.J. **679** (2008) 675.
93) E. Teller, Phys. Rev. **73** (1948) 801.
94) J. Christensen-Dalsgaad, D.O. Gough and M.J. Thompson, Astrophys.J. **378** (1991) 413.
95) D.B. Guenther, L.M. Krauss and P. Demarque, Astrophys.J. **498** (1998) 871.
96) E. Garcia-Berro, S. Torres, L. G. Althaus, I. Renedo, P. Loren-Aguilar, A. H. Corsico, R. D. Rohrmann, M. Salaris, J. Isern, Nature **465** (2010) 194.
97) E. Garcia-Berro, P. Loren-Aguilar, S. Torres, L. G. Althaus and J. Isern, JCAP **1105** (2011) 021.
98) S. E. Thorsett, Phys. Rev. Lett. **77** (1996) 1432.
99) P. Jofré, A. Reisenegger and R. Fernaández, Phys. Rev. Lett. **97** (2006) 131102.
100) T.P. Walker, G. Steigman, D.N. Schramm, K.A. Olive and H.-S. Kang, Astrophys.J. **376** (1991) 51.
101) F.S. Accetta, L.M. Krauss and P. Romanelli, Phys. Lett. **248B** (1990) 146.
102) C. J. Copi, A. N. Davis, L. M. Krauss, Phys. Rev. Lett. **92** (2004) 171301.
103) R. Nagata, T. Chiba and N. Sugiyama, Phys. Rev. D **66** (2002) 103510.
104) R. Nagata, T. Chiba and N. Sugiyama, Phys. Rev. D **69** (2004) 083512.
105) H. Cadendish, Phil. Trans. Roy. Soc. London. **88** (1798) 469.
106) G.T. Gillies, Rep. Prog. Phys. **60** (1997) 151.
107) P.J. Mohr and B.N. Taylor, Rev. Mod. Phys. **72** (2000) 351.

108) J.H. Gundlach and S.M. Merkowitz, Phys. Rev. Lett. **85** (2000) 2869.
109) T.J. Quinn, C.C. Speake, S.J. Richman, R.S. Davis and A. Picard, Phys. Rev. Lett. **87** (2001) 111101.
110) St. Schlamminger, E. Holzschuh and W. Kündig, Phys. Rev. Lett. **89** (2002) 161102.
111) T.R. Armstrong and M.P. Fitzgerald, Phys. Rev. Lett. **91** (2003) 201101.
112) St. Schlamminger, E. Holzschuh, W. Kündig, F. Nolting, R.E. Pixley, J. Schurr, U. Straumann, Phys. Rev. D **74** (2006) 082001.
113) J. Luo et al., Phys. Rev. Lett. **102** (2009) 240801.
114) H.V. Parks and J.E. Faller, Phys. Rev. Lett. **105** (2010), 110801.
115) P.J. Mohr and B.N. Taylor, Rev. Mod. Phys. **77** (2005) 1.
116) P.J. Mohr, B.N. Taylor and D.B. Newell, Rev. Mod. Phys. **80** (2008) 633.
117) J.B. Fixler, G.T. Foster, J.M. McGuirk, M.A. Kasevich, Science, **315**, 74 (2007).
118) G. Lamporesi, A. Bertoldi, L. Cacciapuoti, M. Prevedelli, G.M. Tino, Phys. Rev. Lett. **100** (2008) 050801.
119) R. Thompson, Astron. Lett. **16** (1975) 3.
120) B.E.J. Pagel, *Mon. Not. R. Astron. Soc.* **179** (1977) 81p.
121) P. Tzanavaris et al., Phys. Rev. Lett. **95** (2005) 041301.
122) A. Y. Potekhin et al., Astrophys.J. **505** (1998) 523.
123) A.V. Ivanchik et al., Astron. Lett. **28** (2002) 423.
124) W. Ubachs and E. Reinhold, Phys. Rev. Lett. **92** (2004) 101302.
125) A. Ivanchik et al., Astron. and Astrophys. **440** (2005) 45.
126) E. Reinhold, R. Buning, U. Hollenstein, A. Ivanchik, P. Petitjean, W. Ubachs, Phys. Rev. Lett. **96** (2006) 151101.
127) J. King, J.K. Webb, M.T. Murphy, R.F. Carswell, Phys. Rev. Lett. **101** (2008) 251304.
128) A.L. Malec et al., *Mon. Not. R. Astron. Soc.* **403** (2010) 1541.
129) F. van Weerdenburg, M. T. Murphy, A. L. Malec, L. Kaper and W. Ubachs, Phys. Rev. Lett. **106** (2011) 180802.
130) J. A. King, M. T. Murphy, W. Ubachs and J. K. Webb, arXiv:1106.5786 [astro-ph.CO], to appear in MNRAS.
131) J. Chengalur and N. Kanekar, Phys. Rev. Lett. **91** (2003) 241302.
132) J. Daring, Phys. Rev. Lett. **91** (2003) 011301.
133) J. Daring, Astrophys.J. **612** (2004) 58.
134) N. Kanekar, J. Chengalur, and T. Ghosh, Phys. Rev. Lett. **93** (2004) 051302.
135) N. Kanekar, J. Chengalur, and T. Ghosh, Astrophys.J. **716** (2010) L23.
136) N. Kanekar et al., Phys. Rev. Lett. **95** (2005) 261301.
137) V.V. Flambaum and M.G. Kozlov, Phys. Rev. Lett. **98** (2007) 240801.
138) M.T. Murphy, V.V. Flambaum, S. Muller and C. Henkel, Science, **320** (2008) 161.
139) C. Henkel et al., Astron. and Astrophys. **500** (2009) 725.
140) S.A. Levshakov, A.V. Lapinov, C. Henkel, P. Molaro, D. Reimers, M.G. Kozlov, I.I. Agafonova, Astron. and Astrophys. **524** (2010) 32.
141) P. Jansen, L-H. Xu, I. Kleiner, W. Ubachs, H.L. Bethlem, Phys. Rev. Lett. **106** (2011) 100801.
142) S.A. Levshakov, M.G. Kozlov and D. Reimer, Astrophys.J. **738** (2011) 26.
143) A. Shelkovnikov, R.J. Butcher, C. Chardonnet, A. Amy-Klein, Phys. Rev. Lett. **100** (2008) 150801.
144) A.G. Riess et al., Astron. J. **116** (1998) 1009; S. Perlmutter et al., Astrophys.J. **517** (1999) 565.
145) N. Suzuki *et al.*, arXiv:1105.3470 [astro-ph.CO].
146) Nature **440** (2006) 1094.